

Calibration Issues of Dual-Polarization Radar Measurements

ALEXANDER V. RYZHKOV, SCOTT E. GIANGRANDE, VALERY M. MELNIKOV, AND TERRY J. SCHUUR

Cooperative Institute for Mesoscale Meteorological Studies, University of Oklahoma, Norman, Oklahoma

(Manuscript received 5 April 2004, in final form 10 January 2005)

ABSTRACT

Techniques for the absolute calibration of radar reflectivity Z and differential reflectivity Z_{DR} measured with dual-polarization weather radars are examined herein.

Calibration of Z is based on the idea of self-consistency among Z , Z_{DR} , and the specific differential phase K_{DP} in rain. Extensive spatial and temporal averaging is used to derive the average values of Z_{DR} and K_{DP} for each 1 dB step in Z . Such averaging substantially reduces the standard error of the K_{DP} estimate so the technique can be used for a wide range of rain intensities, including light rain.

In this paper, the performance of different consistency relations is analyzed and a new self-consistency methodology is suggested. The proposed scheme substantially reduces the impact of variability in the drop size distribution and raindrop shape on the quality of the Z calibration. The new calibration technique was tested on a large polarimetric dataset obtained during the Joint Polarization Experiment in Oklahoma and yielded an accuracy of Z calibration within 1 dB.

Absolute calibration of Z_{DR} is performed using solar measurements at orthogonal polarizations and polarimetric properties of natural targets like light rain and dry aggregated snow that are probed at high elevation angles. Because vertical sounding is prohibited for operational Weather Surveillance Radar-1988 Doppler (WSR-88D) radars because of mechanical constraints, the existing methodology for Z_{DR} calibration is modified for nonzenith elevation angles. It is shown that the required 0.1–0.2-dB accuracy of the Z_{DR} calibration is potentially achievable.

1. Introduction

Radar calibration is essential for producing high-quality weather radar data, particularly for rainfall measurements. Most recent reviews of different techniques for the calibration of the radar reflectivity factor Z can be found in Joe and Smith (2001) and Atlas (2002). The reviews concluded that after several decades of research in radar meteorology, we still have serious problems with Z calibration on operational radars. Bolen and Chandrasekar (2000) found variability in the calibrations of the Next Generation Weather Radar (NEXRAD) Weather Surveillance Radar-1988 Doppler (WSR-88D) radars with respect to the National Aeronautics and Space Administration (NASA) Tropical Rainfall Measuring Mission (TRMM) satellite radar that can be used as a traveling standard against which ground-based weather radars can be calibrated. Recent findings of Gourley et al. (2003) also indicate

that the 2–3-dB discrepancy between reflectivities measured by adjacent WSR-88D radars is quite common.

In coming years, many operational weather radars in the United States and other countries will be upgraded by adding a polarimetric capability. Polarization diversity might help to improve the quality of radar reflectivity calibration. Gorgucci et al. (1992, 1999), Goddard et al. (1994), and Scarchilli et al. (1996) expressed the idea that radar reflectivity Z and two polarimetric variables—differential reflectivity Z_{DR} and specific differential phase K_{DP} —are not independent in the rain medium. Therefore, Z can be roughly estimated from Z_{DR} and K_{DP} . The difference between computed and measured values of Z is considered to be a Z bias. Recent studies by Illingworth and Blackman (2002) and Vivekanandan et al. (2003) claim that the accuracy of Z calibration based on the consistency among the three radar variables can be as good as 0.5–1 dB.

Although these findings are encouraging, there are several issues that have to be clarified and resolved prior to practical utilization of the suggested technique. One of them is sensitivity of a “self-consistency” relation to the drop size distribution (DSD) variations and

Corresponding author address: Alexander V. Ryzhkov, CIMMS/NSSL, 1313 Halley Circle, Norman, OK, 73069.
E-mail: alexander.ryzhkov@noaa.gov

uncertainty in raindrop shape and canting. Also, it is not clear how to use this methodology for relatively light precipitation where K_{DP} estimates are very noisy.

The issue of Z_{DR} calibration is crucial for successful applications of a dual-polarization radar. This is also important for implementation of the self-consistency technique that implies unbiased Z_{DR} measurements. Existing methods for Z_{DR} calibration use polarimetric properties of solar radiation or natural weather targets (e.g., Gorgucci et al. 1999; Bringi and Chandrasekar 2001). The latter implies the vertical sounding of light rain. The problem with the operational WSR-88D radars is that the vertical sounding for Z_{DR} calibration cannot be implemented because of mechanical constraints. Hence, the methodology described by Gorgucci et al. (1999) and Bringi and Chandrasekar (2001) should be modified for nonzenith elevation angles. Hubbert et al. (2003) suggest using two cross-polar power measurements from precipitation in addition to solar calibration in order to calibrate Z_{DR} . This technique, however, cannot be utilized for the polarimetric WSR-88D because only one cross-polar component of the radar return is available (Melnikov et al. 2003).

In this paper, we will

- justify required accuracies for Z and Z_{DR} calibration for practical applications;
- examine the limits of the accuracy of Z calibration based on self-consistency by comparing different consistency relations that are available in literature with ours, which were derived from the existing statistics of DSD measurements and polarimetric radar observations in central Oklahoma;
- suggest a new methodology for determining Z bias from the self-consistency relation and provide the results of its testing on a large polarimetric dataset; and
- discuss possible schemes for the absolute calibration of Z_{DR} at nonzenith elevation angles.

Radar data provided in this study were collected with the polarimetric prototype of the WSR-88D radar built at the National Severe Storms Laboratory (NSSL) in 2002 (KOUN WSR-88D radar hereafter). This radar was used for testing the proof of concept of polarimetric NEXRAD during a 1-yr demonstration project referred to as the Joint Polarization Experiment (JPOLE).

2. Required accuracy for Z and Z_{DR} calibration

Polarimetric radars prove to be very efficient for the classification of radar echoes and accurate rainfall estimation. Both tasks require high-quality Z and Z_{DR}

measurements. The accuracy requirements for rain estimation, however, are more stringent than for classification. The most recent version of the polarimetric rainfall estimation algorithm developed at NSSL and tested during JPOLE suggests the combined use of Z , Z_{DR} , and K_{DP} (Ryzhkov et al. 2003, 2005). The following is a description of the proposed algorithm:

$$R = R(Z)/f_1(Z_{DR}), \quad \text{if } R(Z) < 6 \text{ mm h}^{-1}; \quad (1)$$

$$R = R(K_{DP})/f_2(Z_{DR}), \quad \text{if } 6 < R(Z) < 50 \text{ mm h}^{-1}; \quad (2)$$

$$R = R(K_{DP}), \quad \text{if } R(Z) > 50 \text{ mm h}^{-1}; \quad (3)$$

where

$$R(Z) = 1.70 \cdot 10^{-2} Z^{0.714} \quad (\text{standard WSR-88D relation}), \quad (4)$$

$$R(K_{DP}) = 44.0 |K_{DP}|^{0.822} \text{ sign}(K_{DP}), \quad (5)$$

$$f_1(Z_{DR}) = 0.4 + 5.0 |Z_{dr} - 1|^{1.3}, \quad (6)$$

$$f_2(Z_{DR}) = 0.4 + 3.5 |Z_{dr} - 1|^{1.7}. \quad (7)$$

In (4)–(7), Z_{dr} is differential reflectivity expressed in linear units [$Z_{DR}(\text{dB}) = 10 \log(Z_{dr})$], Z is expressed in $\text{mm}^6 \text{ m}^{-3}$, K_{DP} is in deg km^{-1} , and R is in mm h^{-1} . The algorithm implies that Z is used only for light rain ($< 6 \text{ mm h}^{-1}$) and as a general criterion to distinguish different categories of rain intensity, whereas Z_{DR} is needed for the estimation of light and moderate rain. Ryzhkov et al. (2003, 2005) showed that the “synthetic” polarimetric algorithm, defined by (1)–(7), exhibited the best performance among 3 conventional and 17 polarimetric rainfall relations for the JPOLE dataset.

The measurement errors ΔZ and ΔZ_{DR} include biases [$\Delta Z^{(b)}$ and $\Delta Z_{DR}^{(b)}$] and random statistical components [$\Delta Z^{(s)}$ and $\Delta Z_{DR}^{(s)}$]. Statistical properties of $\Delta Z^{(s)}$ and $\Delta Z_{DR}^{(s)}$ depend on a dwell time, the Doppler spectrum width σ_v , the signal-to-noise ratio, and [in the case of $\Delta Z_{DR}^{(s)}$] the magnitude of the cross-correlation coefficient ρ_{hv} between two orthogonal components of the radar signal.

For dwell time corresponding to 48 successive pulses [about 0.1 s for a low pulse repetition frequency (PRF) of 446 Hz and 0.05 s for a high PRF of 1013 Hz, typically used for the KOUN radar], the standard deviation of $\Delta Z^{(s)}$ varies between 1 and 2 dB, depending on σ_v (Bringi and Chandrasekar 2001). Our observations show that typical values of ρ_{hv} in pure rain are within the 0.985–0.995 range at close distances from the radar where the radar resolution volume is relatively small. The theoretical analysis by Bringi and Chandrasekar (2001) and our experimental estimates show that, for

such values of ρ_{hv} and 48 pairs of simultaneous H and V radar samples, the standard deviation of $\Delta Z_{DR}^{(s)}$ is between 0.2 and 0.3 dB.

The impact of statistical errors $\Delta Z^{(s)}$ and $\Delta Z_{DR}^{(s)}$ on the quality of total rain estimates is reduced by spatial and temporal integration of rain rates obtained from (1) and (2). Such reduction does not occur for the Z and Z_{DR} errors resulting from biases $[\Delta Z^{(b)}$ and $\Delta Z_{DR}^{(b)}]$. This means that if the measurement errors of Z and Z_{DR} are solely the result of the biases (caused by wrong calibration, among other factors) then the fractional errors of rain accumulations are the same as fractional errors of rain rates obtained from (1) or (2).

The fractional errors $\varepsilon_{1,2}$ of the rain-rate and rain accumulation estimates caused by biases in Z and Z_{DR} may be calculated from (1) and (2) as

$$\varepsilon_1 = \alpha \Delta Z^{(b)} - \beta_1 \Delta Z_{DR}^{(b)}, \quad (8)$$

$$\varepsilon_2 = -\beta_2 \Delta Z_{DR}^{(b)}, \quad (9)$$

where

$$\alpha = \frac{1}{R(Z)} \frac{dR(Z)}{dZ} \quad \text{and} \quad \beta_{1,2} = \frac{1}{f_{1,2}(Z_{DR})} \frac{df_{1,2}(Z_{DR})}{dZ_{DR}}. \quad (10)$$

Note that measurements of specific differential phase K_{DP} are unbiased and do not require calibration.

It can be easily shown that $\alpha \approx 0.16$, whereas β_1 varies between 1.0 and 1.4 (for $0 < Z_{DR} < 1$ dB) and β_2 varies between 0.83 and 0.90 (for $1 < Z_{DR} < 2$ dB). The limits of Z_{DR} in parenthesis contain average values of Z_{DR} for light rain [$R(Z) < 6 \text{ mm h}^{-1}$] and moderate-to-heavy rain [$6 < R(Z) < 50 \text{ mm h}^{-1}$]. Both β_1 and β_2 decrease with increasing rain intensity and Z_{DR} .

What are acceptable values of ε_1 and ε_2 ? A fractional rms error of the rainfall estimate δ is related to the bias ε and standard deviation σ as

$$\delta^2 = \varepsilon^2 + \sigma^2. \quad (11)$$

The magnitude of σ is determined by the variability of DSDs, statistical measurement errors of radar variables, and other factors. The standard deviation σ represents the accuracy that is potentially achievable if Z and Z_{DR} are ideally calibrated (i.e., $\varepsilon = 0$). It is obvious that a tolerable bias ε should be well below σ .

The fractional errors of polarimetric rainfall estimation at the S band were examined in recent validation studies performed in Florida (Brandes et al. 2002) and in Oklahoma during JPOLE (Ryzhkov et al. 2003, 2005). In Florida, the best polarimetric relation $R(Z, Z_{DR})$ yielded σ equal to 38% for point estimates of the storm rain accumulations. The JPOLE study shows that

the synthetic polarimetric algorithm produces $\sigma = 49\%$ for point hourly totals, and $\sigma = 18\%$ for areal hourly totals if the size of the area is $40 \text{ km} \times 30 \text{ km}$. Generally, the fractional error increases with decreasing rain accumulation. For the JPOLE dataset, σ is 68% for hourly gauge totals G below 5 mm, 38% if $5 < G < 30$ mm, and 22% for $G > 30$ mm, provided that the synthetic algorithm is utilized (Ryzhkov et al. 2005).

If we assume that the accuracy of the Z and Z_{DR} calibration is 1 (in agreement with the NEXRAD Joint System Program Office 1984) and 0.1 dB, respectively, then, according to (8) and (9), $|\varepsilon_1| = 30\%$ and $|\varepsilon_2| = 9\%$ under a worst-case scenario when the biases of Z and Z_{DR} have opposite signs. It follows from (11) that introducing such biases would result in a less than 10% increase in the overall rms error δ for low rain rates or totals ($G < 5$ mm) and a less than 8% increase in the case of moderate-to-heavy rain for which relation (2) is used. Hence, the biases of 1 and 0.1 dB for Z and Z_{DR} are tolerable if the 10% increase in the overall rms error is accepted. Furthermore, we believe that the required accuracy for the Z_{DR} calibration may be relaxed to 0.2 dB for the measurements of moderate-to-heavy rain. Indeed, the magnitude of ε_2 is below 18% for $\Delta Z_{DR}^{(b)} = 0.2$ dB, and the corresponding increase in δ is less than 11% for rain totals between 5 and 30 mm ($\sigma = 38\%$). Such an increase is higher for larger rain totals. However, according to the synthetic algorithm, neither Z nor Z_{DR} are used for the estimation of heavy rain (with $R > 50 \text{ mm h}^{-1}$), which is a major contributor to hourly rain totals exceeding 30 mm.

Such precision of the Z and Z_{DR} calibration (i.e., 1 and 0.1–0.2 dB, respectively) is definitely sufficient for the reliable classification of radar echoes if a multiparameter fuzzy-logic scheme is utilized. There are at least three practically important classification problems that can be solved with a dual-polarization radar: 1) the discrimination between meteorological and nonmeteorological scatterers (ground clutter, insects, and birds), 2) the detection of hail, and 3) the delineation of rain and snow.

The first task imposes very soft requirements for the Z and Z_{DR} calibration because polarimetric contrasts between meteorological and nonmeteorological radar echo are very large. In addition to Z and Z_{DR} , variables such as the cross-correlation coefficient and texture parameters of Z and differential phase Φ_{DP} provide an excellent discrimination capability (Schuur et al. 2003).

The second task (hail detection) requires more accurate measurements of Z and Z_{DR} but they do not have to be as precise as for rainfall estimation. The NSSL's fuzzy-logic algorithm for hail identification utilizes Z , Z_{DR} , ρ_{hv} , and the mean Doppler velocity V . Our clas-

sification analysis showed that if one of the variables Z or Z_{DR} is seriously biased, the remaining radar parameters ensure the correct identification of hail.

Discrimination between stratiform rain and aggregated snow is the most difficult classification task because membership functions for the two hydrometeor classes in the fuzzy-logic formalism overlap heavily. Both classes are characterized by relatively low Z and Z_{DR} , combined with high ρ_{hv} (Ryzhkov and Zrnic 1998). Ryzhkov and Zrnic (2003) recommend detecting melting snow (or bright band) in order to separate the regions of rain and dry snow. High accuracy of the Z and Z_{DR} measurements is not crucial for the detection of the melting zone.

These considerations lead us to the conclusion that, for most important practical applications, the radar reflectivity factor Z should be calibrated with the accuracy of 1 dB, and differential reflectivity Z_{DR} with the accuracy of 0.2 dB. Better accuracy of the Z_{DR} calibration (0.1 dB) might be needed only for measurements of light rain.

3. Calibration of Z based on polarimetric self-consistency

a. A consistency principle

According to the consistency principle, the radar reflectivity factor in rain can be roughly estimated from Z_{DR} and K_{DP} using the following relation:

$$Z = a + b \log(K_{\text{DP}}) + cZ_{\text{DR}}, \quad (12)$$

where Z is expressed in dBZ, Z_{DR} in dB, and K_{DP} in deg km^{-1} . The coefficients a , b , and c in (12) depend on radar wavelength and prevalent raindrop shape, and are supposed to be relatively insensitive to the DSD variations. The consistency principle is formulated in a slightly different way by Goddard et al. (1994) and Illingworth and Blackman (2002). They claim that the ratio of K_{DP} and Z (expressed in $\text{mm}^6 \text{m}^{-3}$) is a well-defined function of Z_{DR} and is virtually independent of DSD variations.

Because K_{DP} can be quite noisy, especially in light rain, Goddard et al. (1994) recommend expressing K_{DP} as a function of Z and Z_{DR} and examining its integral, the total differential phase

$$\Phi_{\text{DP}}^{\text{est}}(R) = 2 \int_0^R K_{\text{DP}}(Z, Z_{\text{DR}}) dr. \quad (13)$$

The radial profile of the measured differential phase Φ_{DP} is then compared to the radial profile of estimated differential phase $\Phi_{\text{DP}}^{\text{est}}$. If the radar is perfectly calibrated, then the two radial profiles should be very close

to each other in the rain medium. The mismatch between these two profiles indicates a possible calibration error of Z . This error can be determined as an adjustment to Z that is required to match the two profiles of the differential phase. This method works only if differential phase is sufficiently large.

Working with the JPOLE polarimetric data we found that, although the idea of the Z calibration based on self-consistency is quite viable, there are serious methodological problems with the practical implementation of this idea in an operational environment. First of all, there are several consistency relations available in the literature. They were obtained with different assumptions about DSDs and raindrop shapes, and produce noticeably different results in the estimation of the Z bias. The discrepancy might point to the fact that the consistency technique is much more affected by uncertainty in DSDs and raindrop shapes than was previously thought.

Another stumbling block is a procedure for “matching” the measured and estimated radial profiles of Φ_{DP} , which was not implicitly described in any of the referred literature sources. It is clear that differential phase should be sufficiently large to make such matching possible. This automatically excludes many rain events with relatively low maximal values of Φ_{DP} (e.g., stratiform or isolated convective precipitation) from the list of suitable targets for such calibration. In the presence of hail, the consistency relations become invalid and this factor further diminishes the number of radials that are appropriate for calibration.

b. Implementation of the consistency principle using area–time integrals

In our study, we suggest a different procedure for the absolute calibration of Z using a self-consistency principle. Instead of examining individual radial profiles of the measured and estimated differential phases Φ_{DP} and $\Phi_{\text{DP}}^{\text{est}}$ according to (13), we calculate area–time integrals of the measured K_{DP} and computed $K_{\text{DP}}(Z, Z_{\text{DR}})$ and match these two integrals by adjusting Z . In practical terms, it is convenient to divide the data collected in a whole spatial/temporal domain into subarrays corresponding to 1-dB increments of radar reflectivity and compute average values of $\langle K_{\text{DP}}(Z) \rangle$ and $\langle Z_{\text{DR}}(Z) \rangle$ as well as a number of data pixels (gates) $n(Z)$ for a given 1-dB interval of Z between Z_{min} and Z_{max} . Following (12), the Z bias is determined by matching the integrals

$$I_1 = \int_{Z_{\text{min}}}^{Z_{\text{max}}} \langle K_{\text{DP}}(Z) \rangle n(Z) dZ, \quad (14)$$

and

$$I_2 = \int_{Z_{\min}}^{Z_{\max}} 10^{-a/b+Z/b-c(Z_{\text{DR}}(Z))/b} n(Z) dZ. \quad (15)$$

Because the consistency relation (12) is valid for rain only, all nonrain echoes should be filtered out prior to comparing I_1 and I_2 .

By integrating specific differential phase over a large space–time domain we substantially reduce the inherent noisiness in the point estimates of K_{DP} and make light rain events (producing very low Φ_{DP}) suitable for polarimetric calibration of Z . Our previous studies showed that the hourly areal rain totals obtained from the $R(K_{\text{DP}})$ algorithm approximate quite well the corresponding estimates from gauges, even for relatively light rain (Ryzhkov et al. 2000, 2003, 2005).

The coefficients a , b , and c in the consistency relation (12) can be obtained using either large statistics of the DSD measurements or polarimetric radar data with well-calibrated Z and Z_{DR} . In both cases, it is instrumental to compute mean values of $\langle K_{\text{DP}}(Z) \rangle$ and $\langle Z_{\text{DR}}(Z) \rangle$ for each 1-dB increment of Z between Z_{\min} and Z_{\max} and to find the coefficients in a multiple linear regression fit

$$Z = a + b \log(\langle K_{\text{DP}}(Z) \rangle) + c \langle Z_{\text{DR}}(Z) \rangle, \quad (16)$$

using different weights given to different Z – $\langle Z_{\text{DR}}(Z) \rangle$ – $\langle K_{\text{DP}}(Z) \rangle$ triplets. The weight for every such triplet is proportional to the product of $\langle K_{\text{DP}}(Z) \rangle$ and the number of data entries corresponding to a particular 1-dB-wide interval of Z . This is logical because the contributions of pixels with different Z to the area–time integral of K_{DP} (measured or computed) depend on Z , and such dependence should be reflected in the weighting function.

c. Sensitivity of the self-consistency equation to the variations of DSD and raindrop shape

We have examined different consistency relations available in the literature and derived our own based on the existing statistics of DSD measurements in central Oklahoma using different assumptions about raindrop shape. A detailed description of the 2D video disdrometer dataset is available (see information online at <http://cimms.ou.edu/~schuur/disdrom/2DVD.html>). We use 25 920 one-minute DSDs measured during a 5-yr period from 1998 to 2004 with the NSSL's 2D video disdrometer (Schuur et al. 2001). The consistency relations that matched with the measured DSDs have been obtained for three dependencies of raindrop shape on their size.

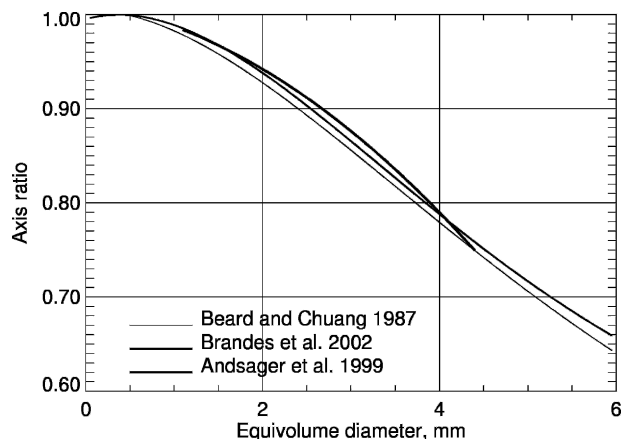


FIG. 1. Different dependencies of the raindrop axis ratio on the equivolume diameter.

In a steady airflow, raindrops have equilibrium shapes as described by Beard and Chuang (1987),

$$r = 1.0048 + 0.00057D - 0.02628D^2 + 0.003682D^3 - 0.0001677D^4, \quad (17)$$

where r is the axis ratio of raindrops and D is its equivolume diameter expressed in mm. The actual shapes of raindrops in unsteady flow are expected to differ from the equilibrium shapes because of drop oscillations. Oscillating drops appear to be more spherical on average than the drops with equilibrium shapes as shown by Andsager et al. (1999) in laboratory studies. They found out that the shape of raindrops in the size range between 1.1 and 4.4 mm is better described by the following formula:

$$r = 1.012 - 0.01445D - 0.01028D^2. \quad (18)$$

Bringi et al. (2003) suggested using Eq. (18) for drops with sizes smaller than 4.4 mm, and Eq. (17) for larger sizes. Another shape–diameter relation that combines the observations of different authors was recently proposed by Brandes et al. (2002),

$$r = 0.9951 + 0.02510D - 0.03644D^2 + 0.005303D^3 - 0.0002492D^4. \quad (19)$$

The dependencies of the raindrop axis ratio on its equivolume diameter for equilibrium shapes defined by (17), “oscillating” raindrop shapes as specified by Bringi et al. (2003), and the ones defined by (19) are shown in Fig. 1.

It was also assumed that the drops are canted with the mean canting angle equal to zero and the width σ of the canting angle distribution of 10° . The coefficients a ,

TABLE 1. Coefficients a , b , and c in (12) for different consistency relations at the S band.

	a	b	c	Assumptions	Source
1	46.4	11.1	1.68	Measured DSD, equilibrium shape	NSSL
2	46.6	10.6	1.91	Measured DSD, Brandes' shape	NSSL
3	49.0	11.7	0.68	Measured DSD, Bringi's shape	NSSL
4	41.9	10.4	2.70	Simulated DSD, equilibrium shape	Gorgucci et al. (1999)
5	45.5	10.0	0.95	Simulated DSD, equilibrium shape	Vivekanandan et al. (2003)
6	42.2	10.0	2.76	Constrained gamma DSD, equilibrium shape	Vivekanandan et al. (2003)
7	44.8	10.0	2.05	Constrained gamma DSD, Brandes' shape	Vivekanandan et al. (2003)
8	39.4	10.0	4.47	Measured DSD, PB shape	Lee and Zawadzki (2004)

b , and c in Eq. (12) for different consistency relations valid at the S band are summarized in Table 1.

In Table 1, constrained gamma DSD means simulated DSD of the gamma form

$$N(D) = N_0 D^\mu \exp(-AD), \quad (20)$$

with parameters Λ and μ related as (Brandes et al. 2003)

$$A = 1.935 + 0.735\mu + 0.0365\mu^2. \quad (21)$$

The "PB" shape in row 8 in Table 1 is a linear dependence of r on D as specified by Pruppacher and Beard (1970)

$$r = 1.03 - 0.062D, \quad (22)$$

if $D > 0.5$ mm, and $r = 1$ otherwise.

To assess limitations on the accuracy of Z calibration resulting from raindrop shape uncertainty and the use of different consistency relations, we performed the following test based on 25 920 DSDs measured with the 2D video disdrometer in Norman, Oklahoma. We computed Z , Z_{DR} , and K_{DP} from measured DSD with three different assumptions about the dependence of raindrop shape on equivolume diameter: equilibrium, Brandes', and Bringi's. Then values of "estimated" reflectivities Z_{est} were calculated from Z_{DR} and K_{DP} using all eight consistency relations with the coefficients listed in Table 1. Average values of $Z_{est} - Z$ in the 30–50-dBZ range are represented in Table 2 for eight algorithms and three assumptions about raindrop shape (columns 2–4).

As can be seen from Table 2, depending on raindrop shape, the results of the Z calibration for any given consistency relation may vary approximately within 1 dB. The difference between Z estimates from different consistency formulas can be as high as almost 4 dB for any particular dependence of the raindrop axis ratio on equivolume diameter. Relations (4) (Gorgucci et al. 1999), (6) (Vivekanandan et al. 2003), and (8) (Lee and Zawadzki 2004) produce the largest errors, at least for Oklahoma.

4. Absolute calibration of Z during JPOLE

a. Radar dataset

A large amount of polarimetric data was collected during JPOLE using the KOUN WSR-88D radar. Radar reflectivities measured by KOUN were regularly compared with the corresponding reflectivity factors obtained from the nearby operational KTLX WSR-88D radar that was supposed to be well calibrated. Because one of the prime objectives of the JPOLE operational demonstration project was validation of polarimetric rainfall measurements, we focused our attention on the 50 km \times 40 km area containing 42 Agricultural Research Service (ARS) Micronet rain gauges (Fig. 2).

For the purposes of this study we identify 43 h of observations when a substantial amount of rain was recorded in the ARS area and simultaneous KOUN and KTLX data were available. These 43 hourly datasets represent 21 separate rain events that occurred between June 2002 and July 2003. For each hour of observation, we obtained estimates of Z , Z_{DR} , K_{DP} , and the cross-correlation coefficient ρ_{hv} with a spatial resolution of 1 km \times 1 km in the 50 km \times 40 km test area with an update time ranging from about 2 min in the year 2002 to 6 min in 2003.

Direct comparisons of the radar reflectivity fields

TABLE 2. Average biases in Z retrieval from different consistency relations and different assumptions about raindrop shape as obtained from the DSD-based simulations (columns 2–4) and radar measurements (column 5). The biases are expressed in dB.

	Equilibrium (DSD)	Brandes' (DSD)	Bringi's (DSD)	Radar measurements
1	-0.03	-0.98	-1.16	0.00
2	0.94	0.00	-0.18	0.86
3	0.92	0.02	-0.11	0.85
4	-2.75	-3.75	-3.96	-2.65
5	-0.49	-1.29	-1.42	-1.19
6	-1.97	-2.94	-3.15	-1.97
7	-0.08	-0.98	-1.17	-0.26
8	-3.04	-4.18	-4.47	-2.32

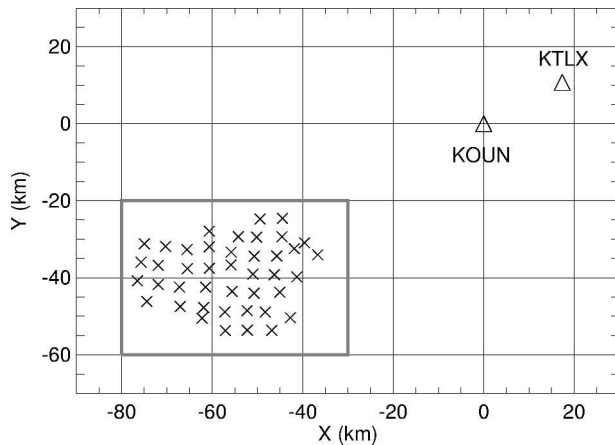


FIG. 2. Radar locations with respect to the 50 km \times 40 km test area enclosed in a rectangle and the ARS Micronet rain gauges (crosses).

measured by the KOUN and KTLX radars have been made to estimate a calibration error of the polarimetric radar. In fact, we estimated hourly rain totals over the ARS area from simultaneous KOUN and KTLX reflectivity data at the 0.5° elevation and calculated the needed adjustment to the Z measurements from the KOUN to match these two estimates. The difference between mean values of Z from KOUN and KTLX ($Z_{\text{KOUN}} - Z_{\text{KTLX}}$ hereafter) varied between -4 and 4 dB; that is, the polarimetric radar was seriously miscalibrated during JPOLE. This could be attributed to the very experimental nature of the prototype. Several microwave components were replaced in the course of the project. Frequent interventions in the microwave assembly by different interested parties made it very difficult to control the radar constant on the daily basis. The RVP7 radar data processor was connected passively to the radar and did not allow for the performance of automatic calibration of Z in the way in which it is normally conducted on operational WSR-88D radars.

The difference $Z_{\text{KOUN}} - Z_{\text{KTLX}}$ for each individual hour was considered as a “ground truth” or “true KOUN miscalibration” against which the self-consistency calibration procedure should be evaluated. Because the consistency method is applicable to the rain medium only, it is necessary to remove the radar data that are contaminated by hail and nonmeteorological scatterers. To filter out pixels with nonrain echoes, we utilize a simple version of the fuzzy-logic classification algorithm that distinguishes between four classes of radar echo: rain, rain/hail mixture, ground clutter/anomalous propagation (AP), and biological scatterers (insects and birds). Three radar variables— Z , Z_{DR} , and ρ_{hv} —are used for classification. A detailed

description of the classification algorithm can be found in Schuur et al. (2003).

b. Relative performance of different consistency relations

Eight consistency relations with the coefficients listed in Table 1 were tested on the JPOLE dataset. We followed the “area-time integration” approach described in section 3b using the 50 km \times 40 km area and 1-h integration time with $Z_{\text{min}} = 30$ dBZ and $Z_{\text{max}} = 50$ dBZ. Prior to the application of the self-consistency technique, the difference of $Z_{\text{KOUN}} - Z_{\text{KTLX}}$ was subtracted from the radar reflectivities measured by the polarimetric radar. Hence, the corrected KOUN reflectivity was assumed to be perfectly calibrated against KTLX, and the consistency method should yield a zero bias if it works appropriately.

Figure 3 displays Z biases (or calibration errors) obtained from the eight relations versus the hour of observations ranked in chronological order. We emphasize that displayed biases represent the difference $Z_{\text{cons}} - Z_{\text{KTLX}}$, where Z_{cons} is the radar reflectivity obtained from the consistency relation and Z_{KTLX} is the reflectivity measured by KOUN and corrected via direct comparisons with KTLX. Ideally, if the KTLX radar is perfectly calibrated and the consistency technique works properly, the difference $Z_{\text{cons}} - Z_{\text{KTLX}}$ would be equal to zero for every hour. In fact, it is not; the discrepancy between Z_{cons} and Z_{KTLX} for individual hours can be larger than 5 dB. Mean values of $Z_{\text{cons}} - Z_{\text{KTLX}}$ averaged over all 43 h for each consistency relation are shown in the right column in Table 2.

Mean Z biases estimated from disdrometer measurements and radar observations agree within 1.3 dB for each consistency relation from Table 1 (except relation 8). This is indirect evidence that (a) the operational KTLX radar was well calibrated and could be served as a good reference, and (b) disdrometer and polarimetric measurements are statistically consistent.

c. Impact of DSD variability

Although the relations (1), (2), (3), and (7) demonstrate relatively good performance, in the sense that the estimates of the $Z_{\text{cons}} - Z_{\text{KTLX}}$ difference averaged over the 1-yr period are less than 1 dB, the errors for individual hours or rain events can be unacceptably high. Deviations from zero for all eight curves in Fig. 3 are well correlated and point to a problem that is common to all consistency relations. We believe that high variability in rain regimes and corresponding drop size distributions observed in Oklahoma are to blame.

Indeed, as radar data show, the mean dependencies

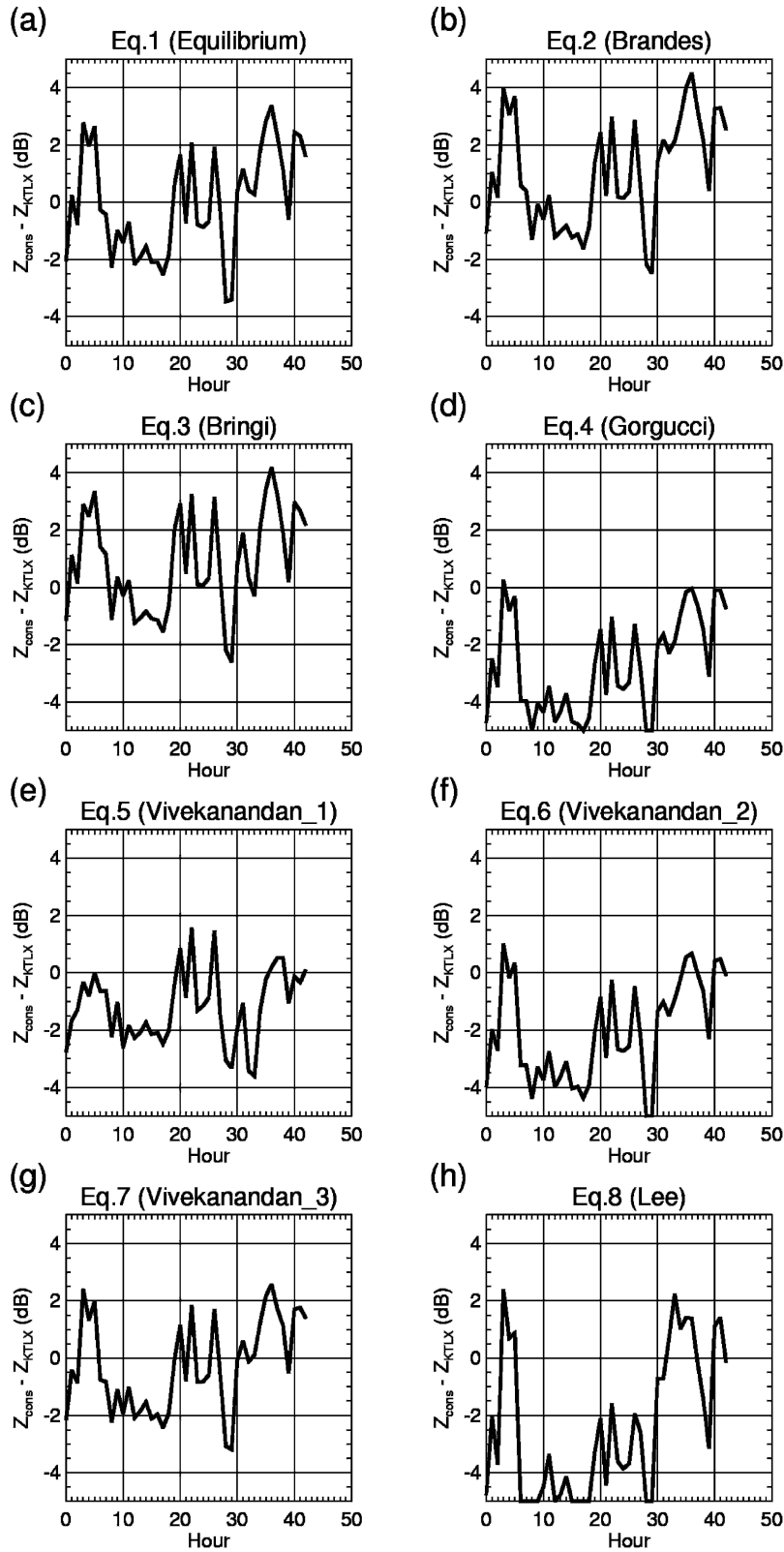


FIG. 3. The differences between the KOUN Z biases estimated from various consistency relations (Z_{cons}) and from direct comparisons with the KTLX radar (Z_{KTLX}) as functions of hour of observations ranked in chronological order.

of Z_{DR} and K_{DP} on Z for individual hours exhibit a very high diversity (Fig. 4). For a given radar reflectivity, Z_{DR} can vary in the 2-dB interval and K_{DP} can change an order of magnitude at lower Z . Two apparent outliers represented by thin curves in Fig. 4 correspond to the case of very large hail on 14 May 2003 when an anomalously high Z_{DR} was measured at the periphery of hail cores in low-reflectivity regions.

After the two outliers were excluded, we divided all hours of observations into two categories: “large drop (LD)” cases (17 h) and “small drop (SD)” cases (24 h). The mean Z - Z_{DR} and Z - K_{DP} dependencies are depicted by thick black lines for LD cases and by thick gray lines for SD cases in Fig. 4. Such division is quite subjective and serves for illustration purposes only. Most convective rain events fall into the “LD category,” whereas the majority of stratiform events that occurred during the fall of 2002 belong to the “SD category.” The average dependencies of Z_{DR} and K_{DP} on Z for the LD and SD categories are plotted in Fig. 5

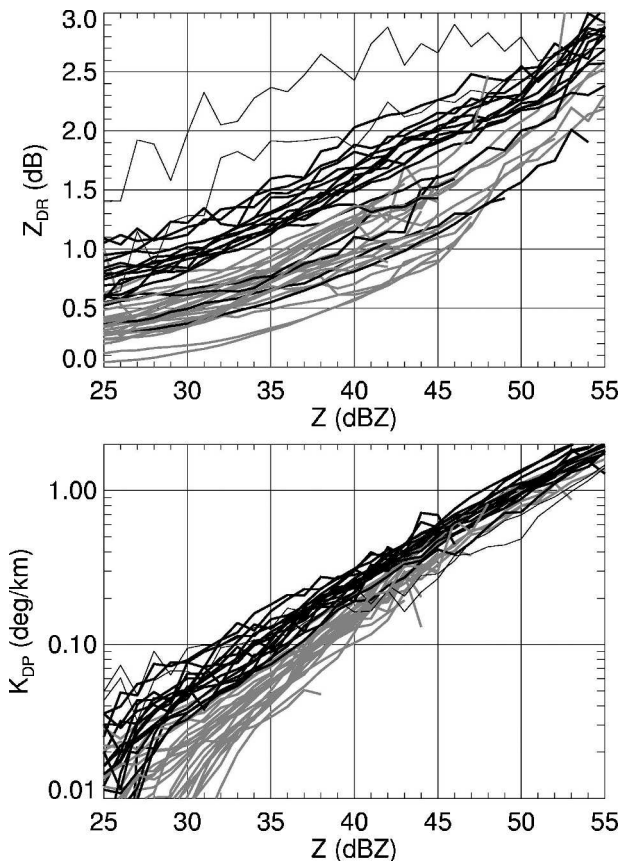


FIG. 4. Mean Z - Z_{DR} and Z - K_{DP} dependencies in the ARS test area for each of the 43 h of JPOLE observations (21 rain events). Thick black curves correspond to the cases with LD rain regimes, thick gray curves to the SD rain regimes, and thin curves to the rain event with large hail.

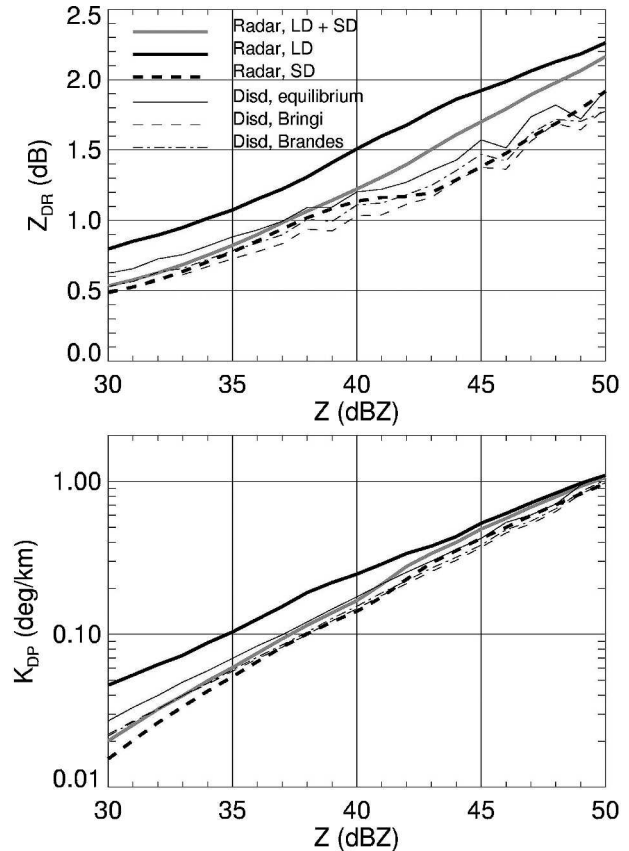


FIG. 5. Mean Z - Z_{DR} and Z - K_{DP} dependencies obtained from the radar for different rain regimes and from the disdrometer for different assumptions about raindrop shapes.

(thick solid and dashed lines). Additional curves in Fig. 5 designate the corresponding average dependencies for all radar data (LD + SD) and for disdrometer data with three different assumptions about raindrop shape.

The three disdrometer curves exhibit more oscillations and are less statistically robust compared to the curves obtained from the radar data, because the disdrometer dataset (25 920 DSDs) is almost two orders of magnitude smaller than the radar dataset. The disdrometer Z - Z_{DR} dependencies agree much better with the SD radar curves than with the LD ones. For reflectivities lower than 40 dBZ, the agreement is also good between the disdrometer data and the overall radar data (LD + SD). This is not surprising because the SD cases are mostly associated with stratiform rain representing the majority of data with Z less than 40 dBZ. A very good match between the radar and disdrometer data at lower reflectivities might also point to the high quality of the Z_{DR} calibration on the KOUN WSR-88D radar.

The difference between the LD and SD types of DSD that is evident in the Z - Z_{DR} and Z - K_{DP} depen-

dencies is also very well pronounced in the $K_{DP}/Z-Z_{DR}$ graph (Fig. 6). This finding drastically contradicts the notion of Goddard et al. (1994) and Illingworth and Blackman (2002) that the ratio of K_{DP} and Z is a universal function of Z_{DR} and is almost independent of DSD variations. Such a claim seems invalid for rain observed in Oklahoma. The consistency relations matched with either the LD or SD curves in Fig. 6 can produce up to a 3–4-dB difference in the estimated Z .

d. Validation of the calibration procedure

Unacceptably high calibration errors of more than 2–3 dB on several occasions during the JPOLE project can be attributed to two major factors. First, the measured values of $\langle Z_{DR}(Z) \rangle$ and $\langle K_{DP}(Z) \rangle$ are very different from the corresponding values that have been used for the derivation of the consistency relations. In other words, the observed DSD does not match well the “average” DSD that is assumed for a particular consistency formula. Second, for very light rain, the area–time domain in (14) and (15) is not large enough to reduce statistical errors in the estimates of the integrals I_1 and I_2 .

We suggest that the following three conditions should be satisfied before the estimate of the Z bias from the polarimetric consistency relation can be accepted.

- 1) There has to be enough rain in the spatiotemporal domain. If the integration in (14) and (15) is performed over $50 \text{ km} \times 40 \text{ km}$ and 1 h, this condition should be expressed as

$$I_1 > 200^\circ \text{ km}^{-1}. \tag{23}$$

- 2) Measured values of $\langle Z_{DR}(Z) \rangle$ and $\langle K_{DP}(Z) \rangle$ after Z correction should be sufficiently close to the corresponding “model” values $\langle Z_{DR}^{(m)}(Z) \rangle$ and $\langle K_{DP}^{(m)}(Z) \rangle$ in (16):

$$\frac{1}{M} \sum_{Z_i=Z_{\min}}^{Z_{\max}} |\langle Z_{DR}(Z_i) \rangle - \langle Z_{DR}^{(m)}(Z_i) \rangle| < 0.20 \text{ (dB)}, \tag{24}$$

$$\frac{1}{M} \sum_{Z_i=Z_{\min}}^{Z_{\max}} |\log \langle K_{DP}(Z_i) \rangle - \log \langle K_{DP}^{(m)}(Z_i) \rangle| < 0.07, \tag{25}$$

where M is a number of the 1-dB increments in the (Z_{\min}, Z_{\max}) interval. Such “quality control” implies that model values of $\langle Z_{DR}^{(m)}(Z) \rangle$ and $\langle K_{DP}^{(m)}(Z) \rangle$ are known. These values are available only for the consistency relations (1)–(3), which we derived ourselves. Therefore, we can check conditions (24) and (25) only for relations (1)–(3). The threshold numbers in (23)–

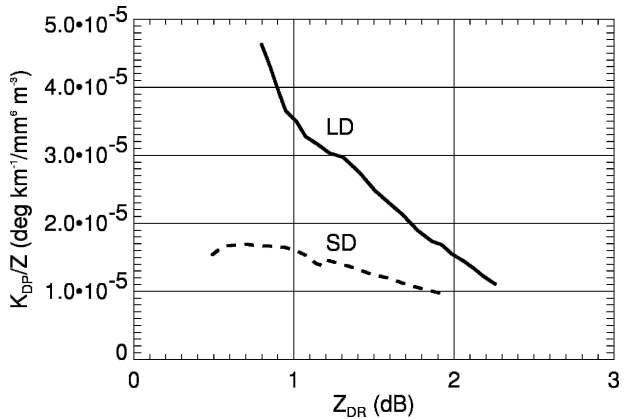


FIG. 6. Mean dependencies of the ratio K_{DP}/Z on Z_{DR} for the LD and SD rain regimes during JPOLE.

(25) were obtained empirically by minimizing the differences $Z_{\text{cons}} - Z_{\text{KTLX}}$ in Fig. 3 down to acceptable levels of 1–2 dB.

Figure 7 illustrates results of the KOUN calibration from direct comparisons of the KOUN and KTLX reflectivities (solid lines) and from the polarimetric consistency provided that conditions (23)–(25) are met (asterisks in Figs. 7a–c). Polarimetric estimates of the Z bias pass the quality control test for 13, 17, and 12 h (out of 43) if the consistency relations (1), (2), and (3) are applied respectively. Overall agreement between the estimates of Z bias from direct radar-to-radar comparisons ($Z_{\text{KOUN}} - Z_{\text{KTLX}}$) and from polarimetric consistency relations (ΔZ_{cons}) is noticeably better after quality control is performed [especially for the relations (2) and (3)]. Reduction of the rms difference between the two estimates is from 1.81 to 1.43 dB for the relation (2) (Brandes’ shape) and from 1.93 to 1.36 dB for the relation (3) (Bringi’s shape).

Additional improvement can be achieved if more than one consistency relation is used. Using radar data collected in the ARS area, and with the methodology described in section 3b, we derived two consistency relations that are matched with the LD and SD rain regimes:

$$Z = 44.0 + 12.2 \log(K_{DP}) + 2.32Z_{DR} \tag{26}$$

for the LD regime, and

$$Z = 46.0 + 9.59 \log(K_{DP}) + 1.68Z_{DR} \tag{27}$$

for the SD regime. Because the LD cases were mostly associated with higher-reflectivity convective rain events and the SD cases with lower-reflectivity stratiform precipitation, the intervals of integration in Eqs. (14) and (15) were slightly different: $Z_{\min} = 35 \text{ dBZ}$

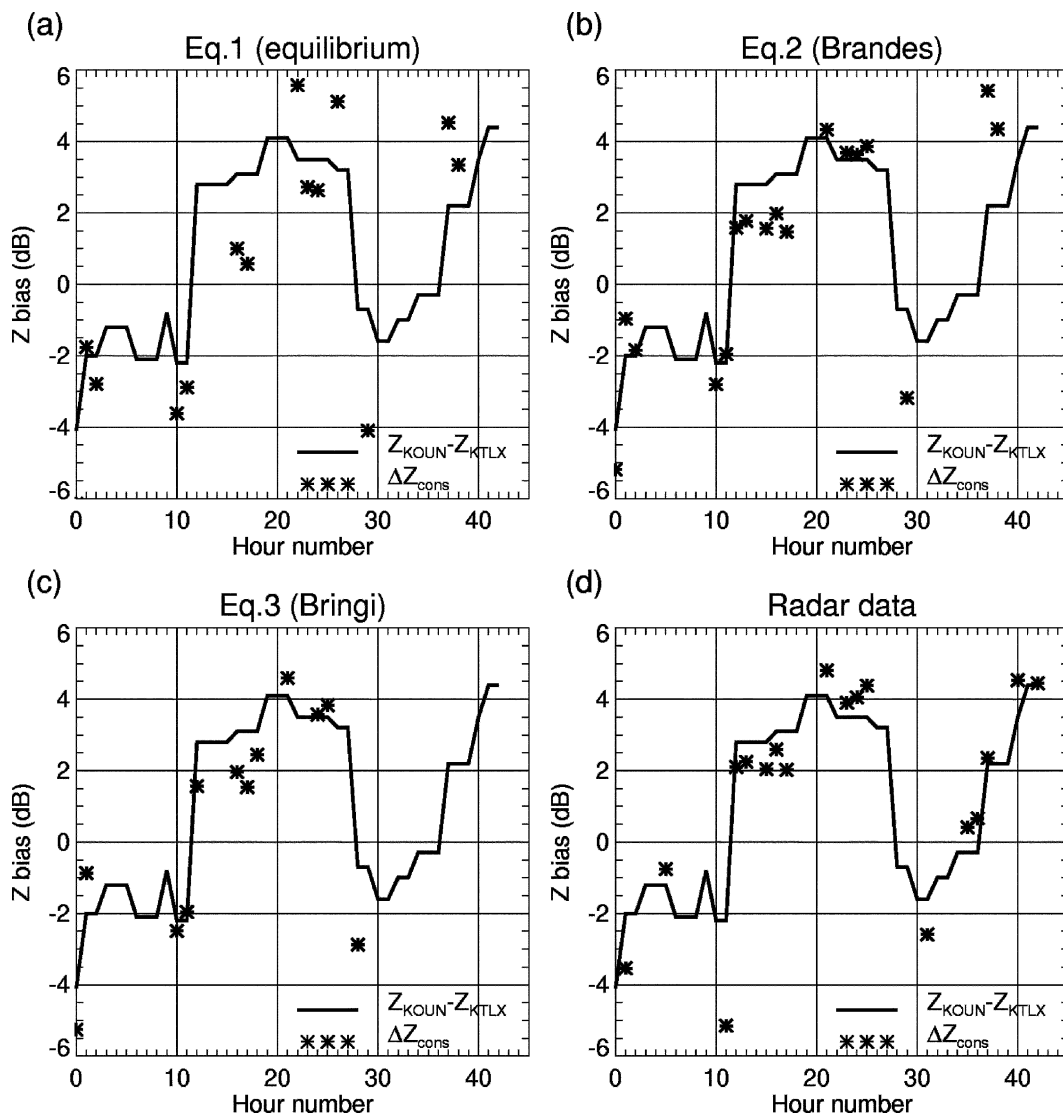


FIG. 7. The bias of reflectivity measurements by the KOUN WSR-88D radar as a function of the hour of observations ranked in chronological order: ΔZ_{cons} is the estimate from the polarimetric consistency method and $Z_{KOUN} - Z_{KTLX}$ is the difference between reflectivities measured by the KOUN and KTLX WSR-88D radars; (a), (b), (c) ΔZ_{cons} from the DSD-based consistency relations is displayed. (d) The corresponding estimate from two consistency relations derived from the radar data is also presented.

and $Z_{max} = 50$ dBZ for the LD relation and $Z_{min} = 30$ dBZ and $Z_{max} = 45$ dBZ for the SD relation.

Consistency relations (26) and (27) were used to compute two estimates of the Z bias for each of the 43 h of observations. Both estimates were subjected to the quality control test using conditions (23)–(25) with model values $\langle Z_{DR}^m(Z) \rangle$ and $\langle K_{DP}^m(Z) \rangle$ that are different for relations (26) and (27). If both estimates passed the quality control, then the one with lower values of the left sides of Eqs. (24) and (25) was accepted. The performance of such calibration procedure is illustrated in Fig. 7d. The $Z_{KOUN} - Z_{KTLX}$ and ΔZ_{cons} estimates

agree better than in Figs. 7a–c, with only one obvious outlier at hour 11. The corresponding rms difference between the two estimates is 1.04 dB (0.77 dB if the outlier at hour 11 is excluded). Thus, application of the two consistency relations has resulted in the increase of valid hourly estimates and their better accuracy.

Strictly speaking, the rms difference between the $Z_{KOUN} - Z_{KTLX}$ and ΔZ_{cons} estimates is not an ideal quality indicator for the polarimetric consistency calibration because the reference KTLX radar might be miscalibrated itself, as it was in the past. However, its possible calibration error is expected to be relatively stable for

long periods of time. An annual trend of the KOUN Z bias in Fig. 7 looks very realistic given the good consistency with the results of polarimetric self-calibration.

e. Self-consistency calibration in light rain

It is important that the suggested polarimetric consistency approach proves to be efficient for light stratiform precipitation observed during the fall of 2002 (hours 12–25 in Fig. 7d). The ARS gauges show that for those hours, an areal mean rain rate varied between 2.0 and 7.3 mm h⁻¹ with an average value of 3.7 mm h⁻¹ that corresponds to $K_{DP} = 0.041^\circ \text{ km}^{-1}$. If we assume that rain with such intensity spreads over 100 km in range, the span of the total differential phase Φ_{DP} barely exceeds 8°. It is difficult to apply the conventional method of matching radial profiles of differential phase with such small Φ_{DP} to reliably estimate the calibration error of Z .

As an example, we illustrate the performance of the conventional and suggested methods for the period from 2200 to 2300 UTC 8 October 2002 when the ARS gauges recorded hourly rain totals of less than 6 mm. The rain type for this event can be characterized as mainly stratiform with embedded convective cells. An hourly dataset contains 29 successive scans of data at elevation 0.5°. Out of 1015 radials of data in the ARS area, we selected the one that contains the largest amount of rain. The corresponding radial profiles of Z , Φ_{DP} , K_{DP} , and ρ_{hv} are displayed in Fig. 8. The maximal value of Φ_{DP} is less than 4° for this particular ray and the whole hourly dataset. Three small convective rain cells with maximal reflectivities exceeding 40 dBZ are evident in the “rain” interval of ranges from 27 to 88 km where $\rho_{hv} > 0.98$. Specific differential phase K_{DP} exhibits pronounced maxima in the two cells between 60 and 80 km from the radar.

Two estimates of specific differential phase K_{DP} are obtained from the filtered Φ_{DP} as a slope of a least squares fit for two range-averaging intervals corresponding to 9 and 25 successive gates. For any particular range gate, the “lightly filtered” estimate of K_{DP} is selected if $Z > 40$ dBZ, and “heavily filtered estimate” is used otherwise (Ryzhkov and Zrníc 1996). Thus, radial resolution of the K_{DP} estimate is about 6 km for relatively light rain ($R < 12$ mm h⁻¹) and about 2 km for more intense rain. The standard deviation in the K_{DP} estimate with 6-km resolution after averaging over 25 gates is about 0.05–0.1° km⁻¹ if the standard deviation of Φ_{DP} is between 1° and 2° and the gate spacing is 0.267 km (Bringi and Chandrasekar 2001). This is confirmed by Fig. 8, which shows that the heavily filtered estimate of K_{DP} in light rain exhibits statistical variations with about a 0.1° km⁻¹ depth.

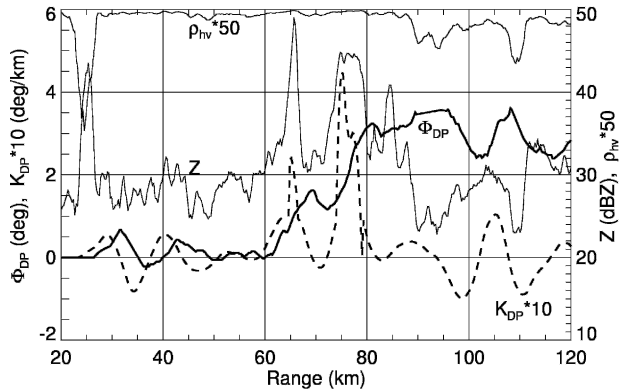


FIG. 8. Radial profiles of Z , K_{DP} , Φ_{DP} , and ρ_{hv} in rain at 2207 UTC 8 Oct 2002 (elevation = 0.5°, azimuth = 231°).

To estimate the Z bias with the accuracy of 1 dB by comparing integrals I_1 and I_2 , the area–time integral of K_{DP} (i.e., I_1) should be estimated with the accuracy of about 20%. This is equivalent to the notion that the standard deviation of the average K_{DP} estimate has to be 0.008° km⁻¹ (if the mean value of K_{DP} is 0.041° km⁻¹), which is much lower than the accuracy of raw estimates of K_{DP} in light rain (0.05–0.10° km⁻¹). The condition (23) stipulates that the integral I_1 should be larger than 200° km⁻¹. This means that at least 5000 estimates of raw K_{DP} must be summed up if average K_{DP} is 0.041° km⁻¹. Of all 5000 estimates of raw K_{DP} , only 200 are statistically independent because we use a 25-gate averaging window to estimate the heavily filtered K_{DP} . Hence, integration of 5000 raw K_{DP} results in $(200)^{1/2} \approx 14$ times reduction in the standard error. Therefore, the standard error of average K_{DP} is between 0.0036 and 0.0072° km⁻¹, which is below the required 0.008° km⁻¹.

A direct comparison of reflectivities (or mean areal rain rates) estimated from the KOUN and KTLX radars indicates that the KOUN radar was 2.8 dB “hotter” than KTLX for this particular day of observations (see Fig. 7). According to the conventional self-consistency methodology, radial dependency of the measured Φ_{DP} from Fig. 8 is compared to the computed $\Phi_{DP}(Z, Z_{DR})$ curves corresponding to different biases in Z (Fig. 9). It appears that the measured and computed Φ_{DP} radial profiles are best matched if the difference between the measured and corrected values of radar reflectivity $\Delta Z_{cons} = 4.5$ dB and the consistency relation (3) from Table 1 or relation (27) are utilized. All other relations from Table 1, as well as Eq. (26) give values of ΔZ_{cons} ranging from 5.0 to 9.5 dB, which are significantly higher than 2.8 dB. The modified approach based on the analysis of area–time integrals yields the estimate of ΔZ_{cons} at 2.0 dB, which is much closer to

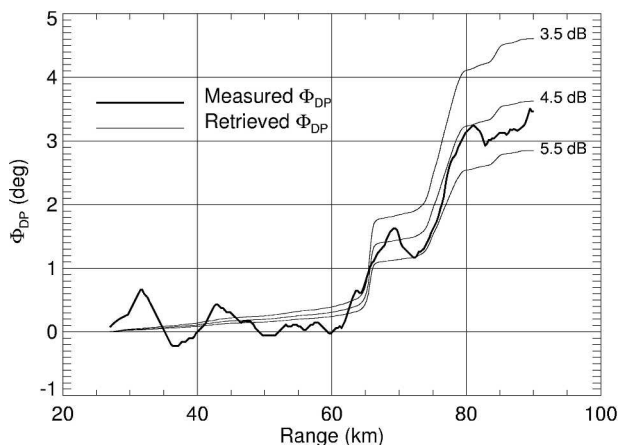


FIG. 9. Radial profiles of the measured and retrieved Φ_{DP} for the ray in Fig. 8. Numbers indicate the magnitude of Z biases corresponding to the three profiles of Φ_{DP} retrieved from observed Z and Z_{DR} according to Eq. (27).

2.8 dB. The algorithm automatically selects the consistency relation (27) as appropriate for this hour and confirms that conditions (23)–(25) are met.

In Fig. 10, the measured dependencies of Z_{DR} and K_{DP} on Z (after 2.0-dB correction) are compared with the corresponding model ones that are associated with the relation (27). It is evident that the measured K_{DP} versus Z dependence does not exhibit any noisiness after averaging over large areal/spatial domain and matches the corresponding model dependency very well. The agreement between the measured and model Z_{DR} curves is not as good, but still satisfies the criterion (24).

The new calibration algorithm gives quite stable values of ΔZ_{cons} between 2.0 and 2.6 dB for successive hours 12–17 when light rain was observed on 8–9 October 2002. These estimates are within 1 dB of the $Z_{KOUN} - Z_{KTLX}$ values obtained from direct comparison of the KOUN and KTLX reflectivities for these hours (Fig. 7d).

5. Absolute calibration of Z_{DR}

The KOUN radar has two separate orthogonal channels to simultaneously transmit and receive radar signals with orthogonal polarizations. Because of the differences in the transmitted powers, microwave losses, and receiver gains and bandwidths between the two channels, one has to control the resulting system bias in differential reflectivity. The reception component of the system bias $Z_{DR}^{(r)}$ can be monitored using solar radiation measurements because the solar radiation has equal powers at horizontal and vertical polarizations.

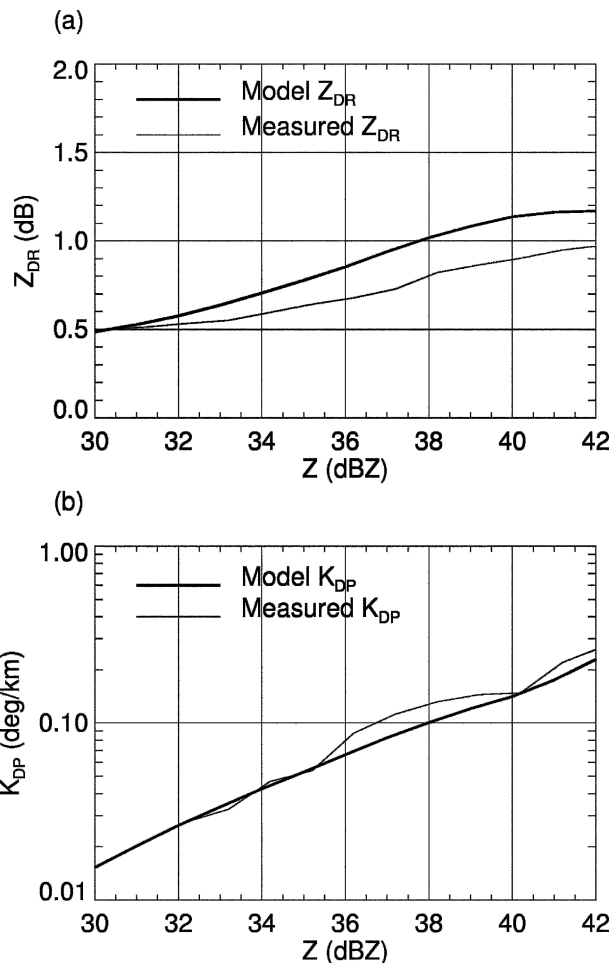


FIG. 10. The Z - Z_{DR} and Z - K_{DP} dependencies after self-consistency calibration of Z is made for the data collected from 2200 to 2300 UTC 8 Oct 2002 (thin lines). The corresponding model dependencies associated with the self-consistency relation (23) are shown by thick lines.

During JPOLE, we regularly used the solar radiation measurements to monitor the stability of $Z_{DR}^{(r)}$. A detailed description of such measurements can be found in Melnikov et al. (2003). Figure 11 gives an idea about the magnitude and stability of $Z_{DR}^{(r)}$ from April to December 2002. The sun-measured $Z_{DR}^{(r)}$ varied within 0.3 dB with a mean value close to -0.3 dB. From our JPOLE experience, a conservative estimate of the accuracy of Z_{DR} calibration using test signals and solar scans is about 0.2 dB. Hubbert et al. (2003) proposed using two cross-polar power measurements that, after combining with solar calibration, might result in better accuracy. However, such a technique is not applicable to the polarimetric WSR-88D because only one cross-polar component of the radar return is available.

The Z_{DR} calibration using solar radiation accurately determines the Z_{DR} system bias on reception but can-

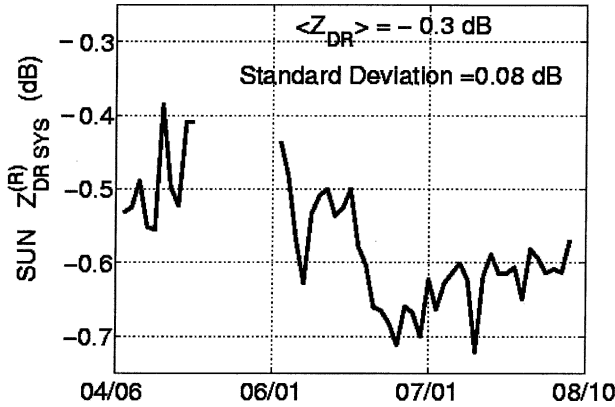


FIG. 11. Time variations of Z_{DR}^r obtained from sun scans during the JPOLE project in 2002.

not account for possible differences in transmitted powers. Although such differences [as well as Z_{DR}^r] could be measured and continually monitored by the polarimetric WSR-88D during data collection, the use of natural calibration targets with known polarimetric properties might provide an alternate way for absolute calibration of Z_{DR} . Measurements at vertical incidence in rain are often used to establish the overall system bias of Z_{DR} (Bringi and Chandrasekar 2001, section 6.3.2). Because the raindrops are symmetrical in the mean for the vertical sounding, the intrinsic Z_{DR} is zero. This method, however, cannot be implemented with the WSR-88D radar because the antenna has a 60° elevation limit determined by the structural configuration of the antenna's pedestal.

Differential reflectivity of weather scatterers decreases with elevation. For oblate spheroidal particles with a mean vertical orientation, this dependence is expressed by the following formula that can be easily derived using theoretical considerations in Bringi and Chandrasekar (2001, sections 2.3.3 and 4.7.1):

$$Z_{DR}(\theta) \approx \frac{Z_{DR}(0)}{[Z_{DR}(0)^{1/2} \sin^2\theta + \cos^2\theta]^2}, \quad (28)$$

where $Z_{DR}(0)$ and $Z_{DR}(\theta)$ are differential reflectivities at elevation angles 0 and θ , respectively. Here Z_{DR} is expressed in a linear scale. Theoretical dependencies of Z_{DR} on elevation angle θ for different $Z_{DR}(0)$ are displayed in Fig. 12. It can be concluded that

$$Z_{DR}(\theta = 60^\circ) \approx 0.24 Z_{DR}(\theta = 0^\circ), \quad (29)$$

where Z_{DR} is expressed in logarithmic units.

Atmospheric scatterers with low variability of intrinsic Z_{DR} at high elevation angles can serve as natural reflectors for Z_{DR} calibration. Our analysis of JPOLE data described in section 4 (see Figs. 4 and 5) shows that

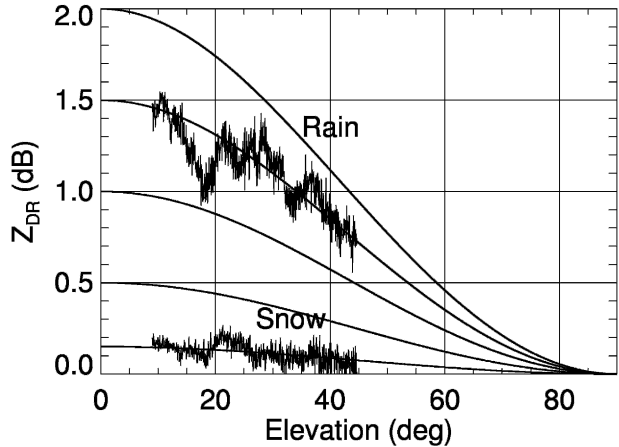


FIG. 12. Measured dependencies of Z_{DR} on elevation angle for rain and snow observed on 7 Apr 2002. Superposed are model dependencies with different Z_{DR} at grazing angles.

light rain is not an optimal target for such calibration because of the high variability of Z_{DR} , even at high elevation angles. Indeed, observational data presented in Fig. 4 indicate that the Z_{DR} of light rain with an intensity between 1 and 5 mm h^{-1} (Z is approximately between 25 and 35 dBZ) varies between 0 and 1.5 dB after we exclude cases with light rain at the periphery of severe hailstorms for which the corresponding Z_{DR} can be as high as 2.3 dB. According to Fig. 12 and (29), this results in the Z_{DR} variability within the 0–0.4-dB interval at an elevation of 60° . Such variability is too high to enable absolute calibration of Z_{DR} with the required accuracy of 0.1–0.2 dB.

Another possible calibration medium is dry aggregated snow that is known for its small intrinsic Z_{DR} resulting from very low density. Our analysis of several snow cases during JPOLE confirms the previous findings by Ryzhkov and Zrnicek (1998) that mean values of Z_{DR} (i.e., averaged over a sufficiently large spatial/temporal interval) in aggregated snow usually do not exceed 0.25 dB and tend to slowly decrease with increasing Z . According to (29), this guarantees that the corresponding variability of Z_{DR} at the 60° elevation will be less than 0.1 dB, which is suitable for the absolute Z_{DR} calibration.

Dry aggregated snow near the surface is not available in many climatic zones. In addition, such a snow type should be carefully separated from wet aggregated snow and dry crystallized snow that are characterized by a much higher and more variable Z_{DR} (Ryzhkov and Zrnicek 1998, 2003). Nevertheless, dry aggregated snowflakes are universally present above the melting layer in stratiform clouds. Numerous polarimetric radar measurements show that Z_{DR} drops almost to zero slightly

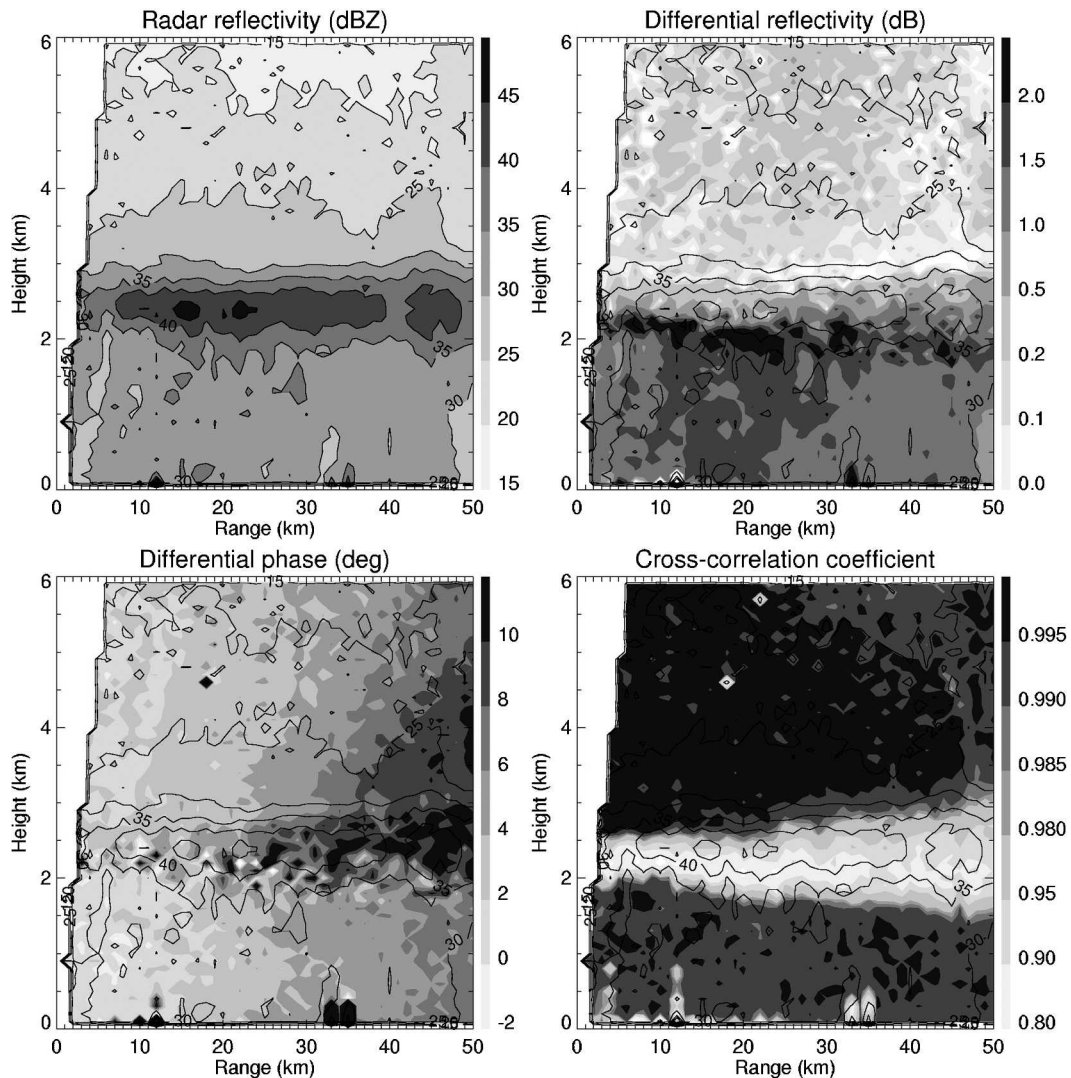


FIG. 13. Composite RHI plot of Z , Z_{DR} , Φ_{DP} , and ρ_{hv} measured with the KOUN WSR-88D radar on 7 Apr 2002.

above the brightband maximum of Z and 0°C level and usually remains close to zero in the 1–2-km layer above (Ikeda and Brandes 2003), where dry aggregated snow is most likely. An example of such vertical dependence is illustrated in Fig. 13, where a composite RHI plot of Z , Z_{DR} , Φ_{DP} , and ρ_{hv} measured with the KOUN WSR-88D radar on 7 April 2002 is presented.

In Fig. 13, the bright band is marked with pronounced signatures in all radar variables, although at slightly different heights. The very bottom of the melting layer is associated with a spike in Z_{DR} , which is followed by the ρ_{hv} minimum in the middle and the Z maximum in the upper parts of the melting layer. All three signatures are below the freezing-level height (0°C). Such vertical dependencies of polarimetric radar

variables in stratiform precipitation are very typical and have been reported in previous studies (e.g., Ryzhkov and Zrnic 1994; Ikeda and Brandes 2003). Notable is a sharp contrast between high values of Z_{DR} in light rain below the bright band (1.0–1.6 dB) and very low values of Z_{DR} in dry aggregated snow above the bright band within the height interval of 2.8–3.8 km (less than 0.20–0.25 dB). Although rain in this example is clearly stratiform, very high Z_{DR} combined with a Z less than 35 dBZ indicate the dominance of large drops in the rain-drop spectrum similar to the cases of moderate-to-severe convection.

The RHI plot in Fig. 13 was obtained using 1000 radials of data collected at elevations between 0° and 45° (i.e., with a very high resolution in the elevation

angle). We examined elevation dependencies of Z and Z_{DR} within the 10° – 45° range for rain below the bright band and dry aggregated snow above the bright band. To avoid contamination from the melting layer, crystals, and ground clutter, we selected range gates corresponding to the height intervals of 1.0–1.8 km for rain and 2.8–3.8 km for snow, provided that ρ_{hv} exceeds 0.99. Mean values of Z and Z_{DR} in rain and snow were computed at each elevation angle. Results of Z_{DR} estimates are superimposed on the model curves in Fig. 12. The observed elevation dependencies of Z_{DR} agree quite well with the model ones for $Z_{DR}(0) = 1.5$ dB in rain and $Z_{DR}(0) = 0.15$ dB in snow. This gives us more confidence that the model (29) adequately describes Z_{DR} as a function of the elevation angle for rain and aggregated snow. The corresponding reflectivities vary between 29 and 34 dBZ in rain and 26 and 29 dBZ in snow with no apparent dependence on the elevation angle.

Finally, we present the Z_{DR} data collected from the 360° azimuthal scans at the elevations of 40° and 60° for the same storm (Fig. 14). The data are displayed at two different heights in snow—3.9 and 4.7 km for 40° and 60° , respectively. Those were minimal heights at which the radar echo was free of ground clutter contamination at all azimuths at the 40° and 60° elevations. Small-scale azimuthal fluctuations of Z_{DR} are a result of statistical variations in the Z_{DR} estimate associated with a relatively short dwell time. Mean values of Z_{DR} are 0.11 and 0.01 dB at the heights of 3.9 (40°) and 4.7 (60°) km, correspondingly.

As Figs. 12–14 show, Z_{DR} in snow above the bright band remains within 0.1–0.2 dB at elevation angles that were much lower than 60° . Hence, absolute calibration of Z_{DR} can be performed at lower than 60° elevation angles, provided that the brightband polarimetric signatures are well defined and differential attenuation is negligible. Smearing effect of a radar beam on the brightband signatures of all radar variables becomes clearly evident at the distances as close as 30–50 km from the radar (Fig. 13). Slightly negative values of Z_{DR} in snow above the melting layer at ranges exceeding 20 km (Fig. 13) are attributed to differential attenuation that is directly proportional to differential phase.

6. Discussion and summary

For most important practical applications of polarimetric weather radar, the radar reflectivity factor Z should be calibrated with the accuracy of 1 dB, and differential reflectivity Z_{DR} with the accuracy of 0.2 dB. Better accuracy of the Z_{DR} calibration (0.1 dB) might be needed for measurements of light rain.

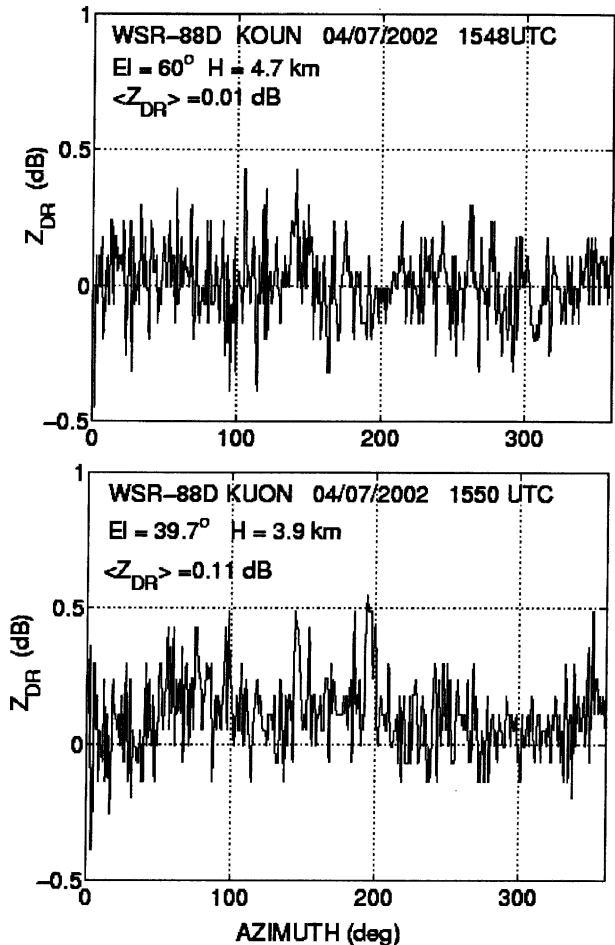


FIG. 14. Azimuthal dependence of differential reflectivity in snow at elevations of (top) 60° and (bottom) 40° for the stratiform precipitation on 7 Apr 2002. The mean values of Z_{DR} are denoted with the angular brackets.

Currently, an automatic “hardware” calibration technique for Z is used on operational WSR-88D radars. This calibration methodology utilizes regular measurements of the transmitted power and test signals to control gains and losses in the receiver. Similar technology is being developed at NSSL to calibrate Z_{DR} in the polarimetric prototype of the WSR-88D. We believe that the automatic hardware methodology, combined with regular solar measurements, will be a primary technique to calibrate Z and Z_{DR} for polarimetric WSR-88D radars. It is strongly recommended, however, that the hardware methodology is complemented by the one that is based on polarimetric properties of natural weather scatterers. The latter methodology can be also automated and implemented “on the fly” in the standard WSR-88D volume coverage pattern (VCP) modes without disrupting data acquisition.

The interdependency between Z , Z_{DR} , and K_{DP} in

rain can be used for the absolute calibration of Z . However, the accuracy of calibration based on self-consistency may be limited because of uncertainties in raindrop shapes and variations of DSD. As our simulations, based on large statistics of measured DSD, show, the raindrop shape uncertainty may result in a 1-dB error in the Z calibration. The impact of DSD variability on the quality of absolute Z calibration is generally stronger, and it was apparently underestimated in previous studies.

To minimize adverse effects of DSD and raindrop shape uncertainties on the quality of radar calibration, we recommend checking how well the measured radar variables Z (after correction), Z_{DR} , and K_{DP} match the corresponding “model” variables that were used for the derivation of the consistency relation. If the diversity of rain regimes and corresponding DSDs is very high (as in Oklahoma) it might be necessary to apply two different consistency relations that are matched with two prevalent types of rain in the area. Only after such measures are applied, one can expect the accuracy of absolute Z calibration to be reduced to 1 dB or lower.

Such an approach allows using any consistency relation, provided that the “model” Z , Z_{DR} , and K_{DP} are known. The consistency relations can be derived from theoretical simulations, disdrometer measurements, or well-calibrated polarimetric radar data (if available). The estimate of the radar constant (or reflectivity bias ΔZ) obtained from any particular consistency relation is accepted only if the measured $Z-\Delta Z$, Z_{DR} , and K_{DP} match sufficiently well the corresponding model values that are associated with this consistency formula.

In operational practice, the radar constant may change abruptly, but will usually remain stable for long periods of time. Therefore, it is usually possible to wait long enough before the appropriate rain type with DSD sufficiently close to a “model” DSD is observed in a sufficiently large spatial/temporal domain.

It is recommended that the estimate of the Z bias should be made by matching area–time integrals of the measured K_{DP} and computed $K_{DP}(Z, Z_{DR})$ rather than matching radial profiles of the measured and calculated differential phases Φ_{DP} . By integrating K_{DP} over a large space–time domain, we substantially reduce inherent noisiness in the point estimates of K_{DP} and make light rain events (producing low Φ_{DP}) suitable for polarimetric calibration of Z .

In addition to the validation study presented in this paper, the modified self-consistency algorithm based on the use of multiple consistency relations and the “area–time integration” approach was implemented in real time and tested for robustness using several JPOLE rain events (Giangrande et al. 2004). The test shows

that variability of the automatically updated bias of Z during individual rain events was within 1 dB.

Two different techniques to calibrate Z_{DR} have been utilized during JPOLE. One is based on regular measurements of solar radiation in the two orthogonal channels. This methodology ensures reliable control of the reception component of the system Z_{DR} bias. Another method uses natural calibration targets with known intrinsic Z_{DR} . It is shown that differential reflectivity of dry aggregated snow is very close to zero at high antenna elevations. This type of snow is commonly present right above the melting layer in stratiform precipitation.

Light rain exhibits much higher variability of Z_{DR} than dry aggregated snow (even at high elevations) and, therefore, may not be considered the best target for calibration of Z_{DR} except for the case of vertical sounding. A vertical sounding, however, cannot be implemented with the WSR-88D radar because the antenna has a 60° elevation limit. Thus, probing snow at high elevation angles is a promising technique for the Z_{DR} calibration for the WSR-88D radars that are planned to be polarized nationwide in the near future. This method provides the accuracy of Z_{DR} calibration within 0.1 dB.

Practical implementation of the suggested method for the calibration of Z_{DR} implies automatic polarimetric detection of the melting layer (Ikeda and Brandes 2003; Giangrande and Ryzhkov 2004) in the standard operational mode of WSR-88D. No special arrangement or disruption of the data collection is necessary.

Acknowledgments. This work would not have been possible without the dedicated support from the NSSL and CIMMS/University of Oklahoma staff who maintain and operate the KOUN polarimetric WSR-88D radar. Dr. Dusan Zrnica provided helpful feedback during the preparation of this manuscript.

The authors would like to acknowledge funding support for this work from the U.S. National Weather Service, the Federal Aviation Administration (FAA), and the Air Force Weather Agency through the NEXRAD Products Improvement Program.

This research is partially in response to requirements and funding provided the FAA. The views expressed are those of the authors and do not necessarily represent the official policy or position of the FAA.

REFERENCES

- Andsager, K., K. V. Beard, and N. F. Laird, 1999: Laboratory measurements of axis ratios for large drops. *J. Atmos. Sci.*, **56**, 2673–2683.
- Atlas, D., 2002: Radar calibration: Some simple approaches. *Bull. Amer. Meteor. Soc.*, **83**, 1313–1316.

- Beard, K. V., and C. Chuang, 1987: A new model for the equilibrium shape of raindrops. *J. Atmos. Sci.*, **44**, 1509–1524.
- Bolen, S. M., and V. Chandrasekar, 2000: Quantitative cross validation of space-based and ground-based radar observations. *J. Appl. Meteor.*, **39**, 2071–2079.
- Brandes, E. A., G. Zhang, and J. Vivekanandan, 2002: Experiments in rainfall estimation with a polarimetric radar in a subtropical environment. *J. Appl. Meteor.*, **41**, 674–685.
- , —, and —, 2003: An evaluation of a drop distribution based–polarimetric radar rainfall estimator. *J. Appl. Meteor.*, **42**, 652–660.
- Bringi, V. N., and V. Chandrasekar, 2001: *Polarimetric Doppler Weather Radar: Principles and Applications*. Cambridge University Press, 636 pp.
- , —, J. Hubbert, E. Gorgucci, W. Randeu, and M. Scoenhuber, 2003: Raindrop size distribution in different climate regimes from disdrometer and dual-polarized radar analysis. *J. Atmos. Sci.*, **60**, 354–365.
- Giangrande, S. E., and A. V. Ryzhkov, 2004: 2004: Polarimetric method for bright band detection. Preprints, *11th Conf. on Aviation, Range, and Aerospace Meteorology*, Hyannis, MA, Amer. Meteor. Soc., CD-ROM, P5.8.
- , —, V. M. Melnikov, and J. Krause, 2004: Calibration of the polarimetric NEXRAD radar using meteorological signals. Preprints, *11th Conf. on Aviation, Range, and Aerospace Meteorology*, Hyannis, MA, Amer. Meteor. Soc., CD-ROM, P5.15.
- Goddard, J., J. Tan, and M. Thurai, 1994: Technique for calibration of meteorological radars using differential phase. *Electron. Lett.*, **30**, 166–167.
- Gorgucci, E., G. Scarchilli, and V. Chandrasekar, 1992: Calibration of radars using polarimetric techniques. *IEEE Trans. Geosci. Remote Sens.*, **30**, 853–858.
- , —, and —, 1999: A procedure to calibrate multiparameter weather radar using properties of the rain medium. *IEEE Trans. Geosci. Remote Sens.*, **37**, 269–276.
- Gourley, J., B. Kaney, and R. Maddox, 2003: Evaluating the calibrations of radars: A software approach. Preprints, *31st Int. Conf. on Radar Meteorology*, Seattle, WA, Amer. Meteor. Soc., 459–462.
- Hubbert, J. C., V. N. Bringi, and D. Brunkow, 2003: Studies of the polarimetric covariance matrix. Part I: Calibration methodology. *J. Atmos. Oceanic Technol.*, **20**, 696–706.
- Ikedo, K., and E. A. Brandes, 2003: Freezing level determination with polarimetric radar: Retrieval model and application. Preprints, *31st Int. Conf. on Radar Meteorology*, Seattle, WA, Amer. Meteor. Soc., 649–652.
- Illingworth, A., and T. Blackman, 2002: The need to represent raindrop size spectra as normalized Gamma distributions for the interpretation of polarization radar observations. *J. Appl. Meteor.*, **41**, 286–297.
- Joe, P., and P. L. Smith, 2001: Summary of the Radar Calibration Workshop. Preprints, *30th Int. Conf. on Radar Meteorology*, Munich, Germany, Amer. Meteor. Soc., 174–176.
- Lee, G. W., and I. Zawadzki, 2004: Errors in radar calibration by gage, disdrometer, and polarimetry: Theoretical limit and application to operational radar. *Proc. Sixth Int. Symp. on Hydrological Applications of Weather Radar*, Melbourne, Australia, Bureau of Meteorology, CD-ROM.
- Melnikov, V. M., D. S. Zrnica, R. J. Doviak, and J. K. Carter, 2003: Calibration and performance analysis of NSSL's polarimetric WSR-88D. NOAA/NSSL Rep., 77 pp. [Available online at http://www.nssl.noaa.gov/88d-upgrades/WSR-88D_reports.html.]
- NEXRAD Joint System Program Office, 1984: Validation phase, part 2 update. NEXRAD Technical Requirements (NTR) Doc. R400A-SP203, 225 pp.
- Pruppacher, H. R., and K. V. Beard, 1970: A wind tunnel investigation of the internal circulation and shape of water drops falling at terminal velocity in air. *Quart. J. Roy. Meteor. Soc.*, **96**, 247–256.
- Ryzhkov, A. V., and D. S. Zrnica, 1994: Observations of MCS with a dual-polarization radar. *Proc. IGARSS'94*, Pasadena, CA, IEEE, 375–377.
- , and —, 1996: Assessment of rainfall measurement that uses specific differential phase. *J. Appl. Meteor.*, **35**, 2080–2090.
- , and —, 1998: Discrimination between rain and snow with a polarimetric radar. *J. Appl. Meteor.*, **37**, 1228–1240.
- , and —, 2003: Discrimination between rain and snow with a polarimetric NEXRAD radar. Preprints, *31st Int. Conf. on Radar Meteorology*, Seattle, WA, Amer. Meteor. Soc., 635–638.
- , —, and R. Fulton, 2000: Areal rainfall estimates using differential phase. *J. Appl. Meteor.*, **39**, 263–268.
- , S. E. Giangrande, and T. J. Schuur, 2003: Rainfall measurements with a polarimetric prototype of the operational WSR-88D radar. Preprints, *31st Int. Conf. on Radar Meteorology*, Seattle, WA, Amer. Meteor. Soc., 208–211.
- , —, and —, 2005: Rainfall estimation with a polarimetric prototype of the WSR-88D. *J. Appl. Meteor.*, **44**, 502–515.
- Scarchilli, G., E. Gorgucci, V. Chandrasekar, and A. Dobaie, 1996: Self consistency of polarization diversity measurements of rainfall. *IEEE Trans. Geosci. Remote Sens.*, **34**, 22–26.
- Schuur, T. J., A. V. Ryzhkov, D. S. Zrnica, and M. Schoenhuber, 2001: Drop size distributions measured by a 2D video disdrometer: Comparison with dual-polarization data. *J. Appl. Meteor.*, **40**, 1019–1034.
- , —, P. Heinselman, D. Zrnica, D. Burgess, and K. Scharfenberg, 2003: Observations and classification of echoes with the polarimetric WSR-88D radar. NOAA/NSSL Rep., 46 pp. [Available online at http://www.nssl.noaa.gov/88d-upgrades/WSR-88D_reports.html.]
- Vivekanandan, J., G. Zhang, S. Ellis, D. Rajopadhyaya, and S. Avery, 2003: Radar reflectivity calibration using differential propagation phase measurement. *Radio Sci.*, **38**, 8049, doi:10.1029/2002RS002676.